Molecular Cell
Article

LincRNA-p21 Activates *p21* In *cis* to Promote Polycomb Target Gene Expression and to Enforce the G1/S Checkpoint

Nadya Dimitrova,[1] Jesse R. Zamudio,[1] Robyn M. Jong,[1] Dylan Soukup,[1] Rebecca Resnick,[1] Kavitha Sarma,[2] Amanda J. Ward,[3] Arjun Raj,[4] Jeannie T. Lee,[2] Phillip A. Sharp,[1] and Tyler Jacks[1,5,*]
[1]Koch Institute for Integrative Cancer Research and Department of Biology, Massachusetts Institute of Technology, 500 Main Street, Cambridge, MA 02142, USA
[2]Department of Molecular Biology, Massachusetts General Hospital, 185 Cambridge Street, Boston, MA 02114, USA
[3]Isis Pharmaceuticals, Inc., 2855 Gazelle Court, Carlsbad, CA 92010, USA
[4]Department of Bioengineering, University of Pennsylvania, 210 South 33rd Street, Philadelphia, PA 19104, USA
[5]Howard Hughes Medical Institute, Massachusetts Institute of Technology, 77 Massachusetts Avenue, Cambridge, MA 02139, USA
*Correspondence: tjacks@mit.edu
http://dx.doi.org/10.1016/j.molcel.2014.04.025

SUMMARY

The p53-regulated long noncoding RNA *lincRNA-p21* has been proposed to act in *trans* via several mechanisms ranging from repressing genes in the p53 transcriptional network to regulating mRNA translation and protein stability. To further examine *lincRNA-p21* function, we generated a conditional knockout mouse model. We find that *lincRNA-p21* predominantly functions in *cis* to activate expression of its neighboring gene, *p21*. Mechanistically, we show that *lincRNA-p21* acts in concert with hnRNP-K as a coactivator for p53-dependent p21 transcription. Additional phenotypes of *lincRNA-p21* deficiency could be attributed to diminished *p21* levels, including deregulated expression and altered chromatin state of some Polycomb target genes, a defective G1/S checkpoint, increased proliferation rates, and enhanced reprogramming efficiency. These findings indicate that *lincRNA-p21* affects global gene expression and influences the p53 tumor suppressor pathway by acting in *cis* as a locus-restricted coactivator for p53-mediated *p21* expression.

INTRODUCTION

The p53 tumor suppressor pathway is activated in the presence of cellular stress, such as DNA damage and oncogenic signaling, and in turn coordinates the transcriptional response of hundreds of genes (Levine and Oren, 2009). Depending on the type of tissue and the nature of the stress signal, p53 activation can initiate multiple pathways that can lead to a temporary pause at a cell-cycle checkpoint to allow for DNA repair, permanent growth arrest (senescence), or cell death (apoptosis) (Vousden and Prives, 2009). It is not clear what determines the outcome of p53 activation. Multiple phenomena, including the strength of p53 binding at the promoters of target genes and the dynamics of p53 oscillations, have been proposed to guide the transcriptional response leading to distinct cellular outcomes (Vousden and Prives, 2009; Purvis et al., 2012).

Based on the identification of mouse long noncoding RNAs (lncRNAs) that are directly induced by p53, recent studies have suggested that lncRNAs may provide an additional layer of transcriptional regulation in the p53 pathway (Guttman et al., 2009; Huarte et al., 2010). Among these, *lincRNA-p21* has been proposed to promote apoptosis (Huarte et al., 2010). Other p53-regulated lncRNAs, including *Pint* and *PANDA*, have been found to antagonize p53 activity by promoting proliferation and by limiting the induction of proapoptotic genes (Hung et al., 2011; Marín-Béjar et al., 2013). In addition, lncRNAs expressed from p53-bound enhancer regions have been found to regulate checkpoint function (Melo et al., 2013a). These studies support a model in which p53-regulated lncRNAs fine-tune the p53 transcriptional response.

In recent years, significant insight has been gained into the numerous mechanisms by which lncRNAs function (Rinn and Chang, 2012). Some well-characterized nuclear lncRNAs, such as *XIST* and lncRNAs expressed from imprinted loci, have been shown to modulate gene expression in *cis* by acting as scaffolds for the recruitment of chromatin-modifying complexes, notably the PRC2 complex, and by altering the chromatin structure of target genes (Lee and Bartolomei, 2013). Other *cis*-acting lncRNAs, such as enhancer RNAs (eRNAs), have been suggested to activate gene expression by locally regulating chromatin architecture (Melo et al., 2013b). In contrast, a growing class of lncRNAs, including *lincRNA-p21*, has been proposed to regulate gene expression in *trans* by directing the chromatin localization of protein binding partners (Fatica and Bozzoni, 2014). Finally, a class of cytosolic lncRNAs, including human *lincRNA-p21*, has been proposed to regulate mRNA translation and protein stability (Yang et al., 2014; Yoon et al., 2012).

Here, we have investigated the effects of *lincRNA-p21* deficiency on the control of expression of p53 target genes and on the p53-dependent cellular response in cells, derived from a *lincRNA-p21* conditional knockout mouse model. Our findings

differ significantly from previous studies, which used RNAi to deplete *lincRNA-p21* levels, and highlight the advantages of using a genetic system to study the function of low copy number, *cis*-acting lncRNAs. The data presented here reveal a mechanism for regulation in the p53 tumor suppressor network, whereby *lincRNA-p21* acts as a transcriptional coactivator that locally reinforces *p21* activation past a functional threshold.

RESULTS

Generation of *lincRNA-p21* Conditional Knockout Mice and Cells

To investigate the role of *lincRNA-p21* in vivo, we mutated the *lincRNA-p21* locus using a conditional gene targeting strategy. The targeting design was directed at preventing expression of the *lincRNA-p21* transcript by flanking the promoter region, which includes the p53 response element (p53RE) as well as the first exon of *lincRNA-p21*, with loxP sites (see Figures S1A and S1B online). *LincRNA-p21*-deficient animals are viable, born at Mendelian ratios, and display no significant abnormalities or predisposition to tumor development by the age of 18 months (Figures S1A–S1E).

To characterize the function of *lincRNA-p21*, we isolated primary mouse embryonic fibroblasts (MEFs) from littermate E13.5 embryos with *lincRNA-p21*$^{-/-}$ and *lincRNA-p21*$^{+/+}$ genotypes, as well as *lincRNA-p21*$^{f/f}$; *Rosa26-CreER*^{T2} MEFs, in which *lincRNA-p21* deletion could be induced by treatment with tamoxifen. Loss of *lincRNA-p21* expression was confirmed by quantitative RT-PCR (qRT-PCR) and RNA-seq (Figures S1F–S1H).

Deletion of *lincRNA-p21* Affects Gene Expression Globally

To examine the role of *lincRNA-p21* in the regulation of gene expression, we performed global expression analysis. RNA was collected from three independent pairs of littermate *lincRNA-p21*$^{+/+}$ and *lincRNA-p21*$^{-/-}$ MEFs, harvested from untreated cells and at 24 hr following treatment with the DNA damage-inducing agent doxorubicin. To identify *lincRNA-p21*-responsive genes, we set a stringent classification in which high-confidence differentially expressed genes (FDR < 0.05) were required to show consistent variation of 34% or more (|log 2 fold change| > 0.43) in all three *lincRNA-p21*-deficient samples compared to the corresponding littermate wild-type controls.

In the absence of DNA damage, we identified a set of 143 genes that were differentially expressed between *lincRNA-p21*-proficient and -deficient samples (Figure 1A, left; Table S1). To recognize statistically significant correlations with curated gene sets within the Molecular Signature Database (MSigDB), we performed gene set enrichment analysis (GSEA) and identified 122 gene sets affected by *lincRNA-p21* loss (FDR < 0.0001; Table S2) (Subramanian et al., 2005). Connectivity maps revealed a pattern associated with increased proliferation mediated by cell-cycle regulators (Figure 1C, top). We also noted that the cyclin-dependent kinase inhibitor *p21* (also known as CDKN1a/Cip1/WAF1), located 16.7 Kb upstream of *lincRNA-p21*, was one of the differentially expressed genes. *p21* is a direct target of p53 transcriptional regulation that is induced upon passaging of primary cell cultures as well as in response to cellular stress and acts to arrest cell-cycle progression at the G1/S checkpoint (Deng et al., 1995; Brugarolas et al., 1995). *p21* expression levels were reduced in all three *lincRNA-p21*-deficient MEF lines compared to wild-type controls (Figure S2C; Table S1). The roles of *lincRNA-p21* in cell-cycle control and in promoting the expression of *p21* will be examined in more detail below.

Using an identical approach, we next singled out 904 genes whose expression levels were significantly altered in *lincRNA-p21*-deficient samples compared to wild-type controls following doxorubicin-induced DNA damage (Figure 1A, right; Figure 1B; and Table S1). Enrichment map summaries of the differentially expressed genes revealed correlations with gene sets related to the doxorubicin response and the p53 pathway (Figure 1C, bottom; FDR < 0.0001; and Table S2). Strikingly, GSEA also uncovered a negative correlation with multiple gene sets associated with the Polycomb Repressive Complex 2, PRC2 (Figure 1C). In fact, pathway analysis using only the 649 genes that were downregulated in the doxorubicin-treated, *lincRNA-p21*-deficient samples indicated a strong overlap with PRC2 function. Seven out of the top 12 MSigDB Chemical and Genetic Perturbations (CGP) categories represented gene sets whose promoters were either occupied by components of the PRC2 complex (Eed and Suz12) or carried the Polycomb chromatin signature (H3K27me3) in various cell types (Figure 1D). The PRC2 complex, which plays an essential role in the epigenetic silencing of regulatory genes controlling differentiation during embryonic development (Aldiri and Vetter, 2012), has not previously been implicated in the DNA damage response or in the p53 pathway. However, multiple reports have shown important regulatory functions of lncRNAs in the PRC2 pathway (Davidovich et al., 2013; Kaneko et al., 2013; Khalil et al., 2009; Zhao et al., 2010).

Of note, comparison of the *lincRNA-p21*-dependent genes identified here with the previously published *lincRNA-p21*-regulated gene set (Huarte et al., 2010) showed no significant overlap, despite the similarity in cell type (MEFs) and treatment (doxorubicin) (Figures S2A–S2C). This discrepancy is likely due to the different methods used to downregulate *lincRNA-p21* (potent genetic deletion versus RNAi-based posttranscriptional knockdown) and highlights the importance of complementary genetic approaches to functional studies.

LincRNA-p21 Promotes the Expression of a Set of DNA Damage-Inducible, PRC2-Target Genes

Since PRC2 targets (defined by Benporath_PRC2_Targets gene set) were significantly enriched in the *lincRNA-p21*-responsive gene set (Table S3), we investigated this connection further, anticipating that these studies might shed light on the role of lncRNAs in the regulation of Polycomb function. We observed that the majority of these genes were lineage-specific transcription factors, whose expression is expected to be repressed by Polycomb in primary MEFs and whose induction may be facilitating the activation of a wider transcriptional response. Indeed, the expression of several genes selected from this set was not detectable by qRT-PCR and by western blotting in untreated samples (Figure 2A). However, these genes became strongly upregulated at 24 hr following doxorubicin treatment, and this

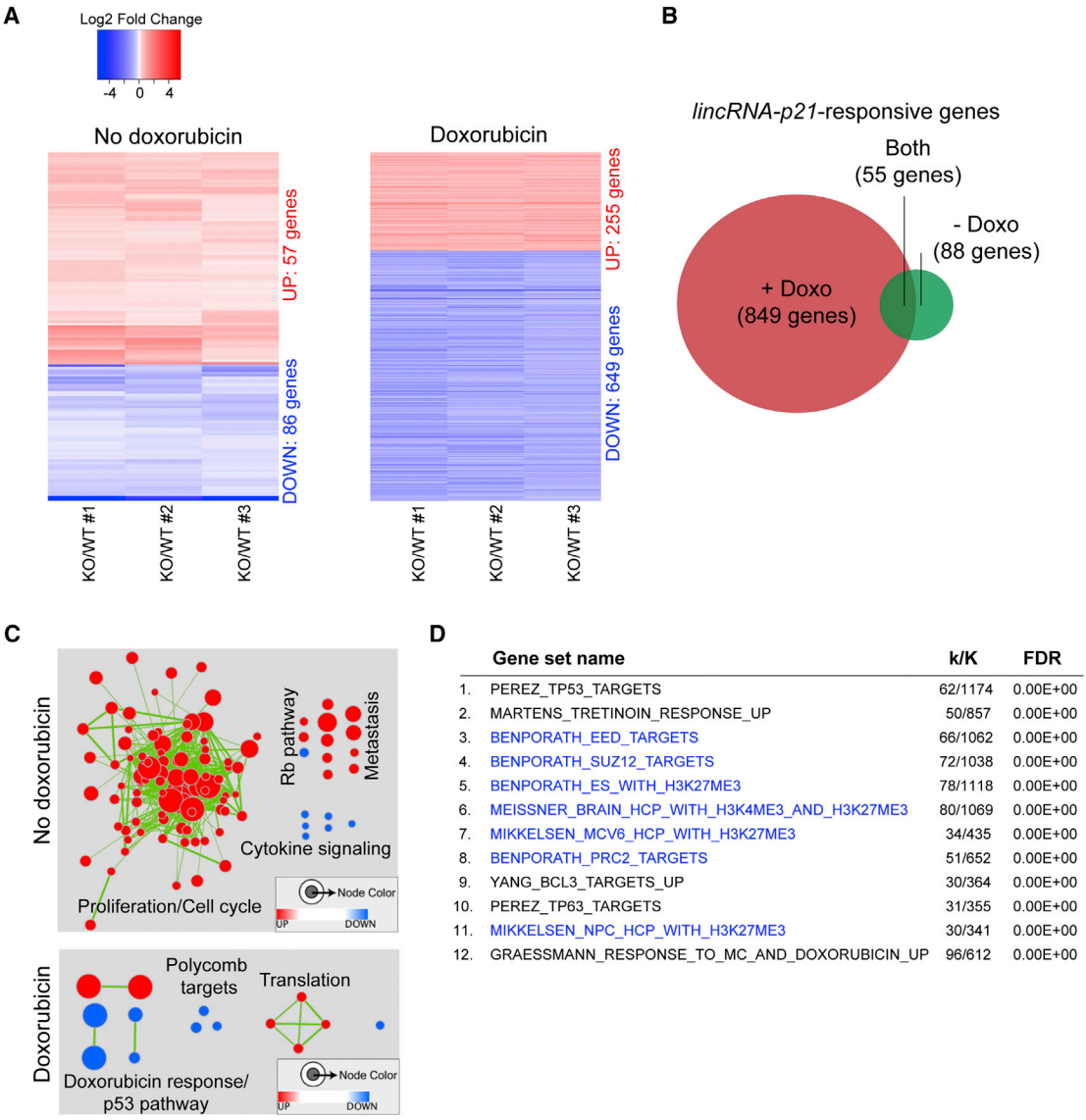

D

	Gene set name	k/K	FDR
1.	PEREZ_TP53_TARGETS	62/1174	0.00E+00
2.	MARTENS_TRETINOIN_RESPONSE_UP	50/857	0.00E+00
3.	BENPORATH_EED_TARGETS	66/1062	0.00E+00
4.	BENPORATH_SUZ12_TARGETS	72/1038	0.00E+00
5.	BENPORATH_ES_WITH_H3K27ME3	78/1118	0.00E+00
6.	MEISSNER_BRAIN_HCP_WITH_H3K4ME3_AND_H3K27ME3	80/1069	0.00E+00
7.	MIKKELSEN_MCV6_HCP_WITH_H3K27ME3	34/435	0.00E+00
8.	BENPORATH_PRC2_TARGETS	51/652	0.00E+00
9.	YANG_BCL3_TARGETS_UP	30/364	0.00E+00
10.	PEREZ_TP63_TARGETS	31/355	0.00E+00
11.	MIKKELSEN_NPC_HCP_WITH_H3K27ME3	30/341	0.00E+00
12.	GRAESSMANN_RESPONSE_TO_MC_AND_DOXORUBICIN_UP	96/612	0.00E+00

Figure 1. Loss of *lincRNA-p21* Affects Gene Expression Globally

(A) Heatmaps of differentially expressed genes (Table S1) in untreated (left) and doxorubicin (Doxo)-treated (right) pairs of littermate *lincRNA-p21*-proficient (WT) and -deficient (KO) MEFs, FDR < 0.05, |log 2 fold change KO/WT| > 0.43 in all three biological replicates.

(B) Venn diagram of the overlap of the *lincRNA-p21*-reponsive genes in the presence and absence of doxorubicin (Doxo).

(C) Connectivity maps of gene sets based on GSEA of differentially expressed genes in (A) (Table S2; FDR < 0.0001). Red nodes represent enrichment with loss of *lincRNA-p21*, and blue represents enrichment in wild-type cells. Node size reflects the number of genes in each set, and edge thickness reflects the overlap between the sets.

(D) Top 12 categories of GSEA of 649 *lincRNA-p21*-responsive, doxorubicin-regulated genes using the CGP Collection of MSigDB. Gene sets related to the PRC2 pathway are highlighted in blue. k indicates the number of *lincRNA-p21*-responsive genes; K represents the number of genes included in a given gene set.

See also Figures S1 and S2, Table S1, and Table S2.

induction was in part dependent on *lincRNA-p21* (Figures 2A, S3A, and S3B). Global expression analysis and qRT-PCR validation indicated that the effect of *lincRNA-p21* deficiency was limited to a subset of PRC2 target genes (Figures S3B and S3C). Importantly, since *lincRNA-p21* is a p53-regulated gene, we confirmed that the expression of this set of genes was also dependent on the p53 status (Figure 2B), even though p53-binding sites were not identified in the promoters of these genes (data not shown). Moreover, induction of several of these genes could also be observed under other conditions that led to p53-dependent *lincRNA-p21* expression, such as in response to oncogenic stress following restoration of p53 expression in a lung adenocarcinoma cell line (Figure S3D) (Feldser et al., 2010). These data suggested an unanticipated connection between the p53-mediated stress response, *lincRNA-p21*, and Polycomb-regulated genes.

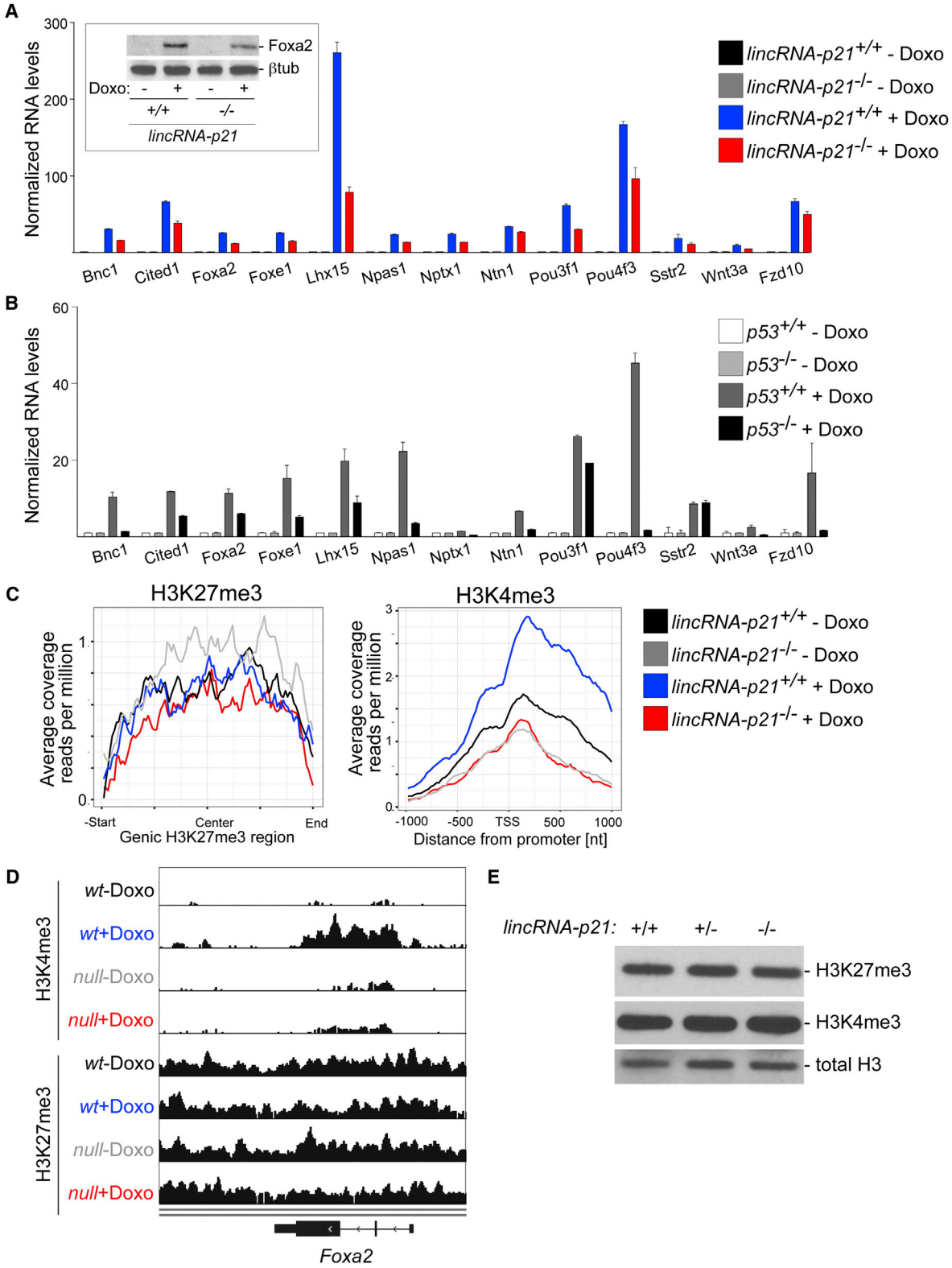

Figure 2. *LincRNA-p21* Promotes the Expression and Influences the Chromatin State of a Set of DNA Damage-Inducible, PRC2-Target Genes
(A and B) qRT-PCR analysis of selected *lincRNA-p21*-responsive, PRC2 target genes in indicated MEFs and treatments. Data, replicated in >3 independent experiments, are represented as mean ± SEM of technical replicates. (Inset) Immunoblot analysis of Foxa2.

(legend continued on next page)

LincRNA-p21 Influences the Chromatin State of Polycomb Target Genes

We next sought to determine the mechanism by which *lincRNA-p21* regulated this subset of PRC2 target genes. To test whether *lincRNA-p21* regulated the chromatin state of its responsive Polycomb target genes, we performed H3K27me3 and H3K4me3 ChIP-seq in *lincRNA-p21*$^{+/+}$ and *lincRNA-p21*$^{-/-}$ MEFs, harvested at 24 hr following mock or doxorubicin treatment. Meta-analysis of the loci of the *lincRNA-p21*-regulated, PRC2 target gene set revealed that the PRC2-specific H3K27me3 modification was not affected by the doxorubicin treatment or by *lincRNA-p21* deficiency (Figures 2C and S4A). In contrast, whereas the activating H3K4me3 mark increased in wild-type cells in the presence of DNA damage, it remained unchanged following doxorubicin treatment in *lincRNA-p21*$^{-/-}$ MEFs (Figures 2C, 2D, and S4A). Importantly, the effect of *lincRNA-p21* deficiency did not lead to global changes in chromatin state (Figures 2E and S4B), and not all loci subject to Polycomb regulation were affected (Figure S4C). These data suggested that *lincRNA-p21* status influenced the expression of a subset of DNA damage-inducible, PRC2 target genes by affecting positive regulators associated with transcriptional activation, which, in these cases, appeared to override the persistent H3K27me3 repressive mark.

LincRNA-p21 Indirectly Regulates PRC2 Target Genes via *p21*

We speculated that *lincRNA-p21* may regulate the expression of the subset of PRC2 target genes by exerting a global effect on chromatin regulation. However, by RNA immunoprecipitation, we found no evidence for an interaction between *lincRNA-p21* and components of the repressive PRC2 complex or other chromatin modifiers (Huarte et al., 2010; data not shown). Moreover, the relatively low stability of *lincRNA-p21* (half-life < 2 hr) and its low copy number (~8 molecules/cell in the presence of DNA damage) were not consistent with a functional role as a widespread *trans*-regulator (Figures S5A and S5B). We next considered the possibility that *lincRNA-p21* may directly bind at the promoters of PRC2 target genes and locally regulate the chromatin state at these sites. However, by single-molecule RNA fluorescent in situ hybridization (RNA FISH), we did not observe colocalization between *lincRNA-p21* RNA and a set of probes specific to the intron of the *lincRNA-p21*-responsive, PRC2 target gene *Ntn1*, designed to indicate the transcription site of this gene (Figure S5C). These data suggested that *lincRNA-p21* did not physically interact with the loci of PRC2 target genes.

We therefore examined the possibility that *lincRNA-p21* may affect the expression of PRC2 target genes indirectly. Since several reports have linked *p21* and cellular differentiation (Missero et al., 1996; Steinman et al., 1994; Zhang et al., 1999), we speculated that the reduction of *p21* levels observed by RNAseq in *lincRNA-p21*-deficient cells (Table S1) might contribute to the deregulation of the PRC2 target genes. Indeed, by qRT-PCR we found that all the examined *lincRNA-p21*-regulated, PRC2 target genes showed reduced induction levels following doxorubicin treatment in *p21*-deficient MEFs compared to wild-type controls (Figure 3A). Moreover, by ChIP-qPCR we detected a reduction in the H3K4me3 chromatin mark and no change in the H3K27me3 chromatin modification at the promoters of *Foxa2*, *Npas1*, and *Pou4f3*, three genes randomly selected from the set of *lincRNA-p21*-responsive, PRC2 targets (Figure 3B). These data indicated that *lincRNA-p21* and *p21* played similar roles in promoting the DNA damage-dependent induction of the identified set of PRC2 target genes.

To establish whether *lincRNA-p21* and *p21* acted in the same pathway, we performed an epistasis experiment. We downregulated *p21* in *lincRNA-p21*$^{+/+}$ and *lincRNA-p21*$^{-/-}$ MEFs using a lentiviral short hairpin RNA (shRNA), which led to a greater than 90% knockdown of *p21* (Figure 3C). A luciferase-specific hairpin was used as a negative control. We found that both *lincRNA-p21* deficiency and *p21* knockdown led to diminished DNA damage-dependent induction of *Foxa2*, *Npas1*, and *Pou4f3* (Figure 3D). Importantly, combined loss of *lincRNA-p21* and *p21* did not further exacerbate the effect (Figure 3D). Based on these findings, we concluded that the *lincRNA-p21*-dependent transcriptional induction of a subset of PRC2 target genes in response to genotoxic stress was mediated through its control of *p21*.

LincRNA-p21 Activates the Expression of *p21*

We therefore sought to dissect the role of *lincRNA-p21* in the regulation of its neighboring gene, *p21* (Figure 4A). By qRT-PCR, we confirmed that acute, tamoxifen-mediated depletion of *lincRNA-p21* from *lincRNA-p21*$^{f/f}$; *Rosa26-CreER*^{T2} MEFs resulted in a reproducible 30%–50% decrease of *p21* RNA and protein levels over two to three cell divisions (Figures 4B and 4C). The effect appeared specific to *p21*, since loss of *lincRNA-p21* did not affect the expression of the gene distal to *lincRNA-p21*, *Srsf3*, and did not lead to a general defect in the activation of the p53 pathway (Figure 4B; data not shown).

We next asked whether the p53-dependent induction of *p21* in response to DNA damage was affected by *lincRNA-p21* deficiency. We observed that in *lincRNA-p21*$^{-/-}$ MEFs treated with γ-irradiation or doxorubicin, *p21* was induced with the same kinetics as in wild-type cells but that the total *p21* RNA and protein levels remained significantly reduced by 30%–50% compared to control cells (Figures 4D–4G and S6A). These data indicated that *lincRNA-p21* positively regulates *p21* levels in passaged primary MEFs and in response to genotoxic stress.

The region of deletion in *lincRNA-p21*-deficient cells is located 16.7 Kb upstream of the *p21* transcription start site and contains binding sites for multiple transcription factors, including p53 (Huarte et al., 2010), as well as chromatin features that are associated with both promoter and enhancer regions. Therefore, it

(C) Metaplots of the genic H3K27me3 (left) and promoter-associated H3K4me3 (right) ChIP-seq enrichment levels at *lincRNA-p21*-responsive, PRC2 target genes in indicated MEFs and treatments.

(D) Genome browser snapshot of *Foxa2* locus, related to ChIP-seq in (C).

(E) Immunoblot analysis of H3K4me3 and H3K27me3 protein levels in whole-cell extracts of doxorubicin-treated MEFs. Total H3 was used as a loading control. See also Figures S3 and S4 and Table S4.

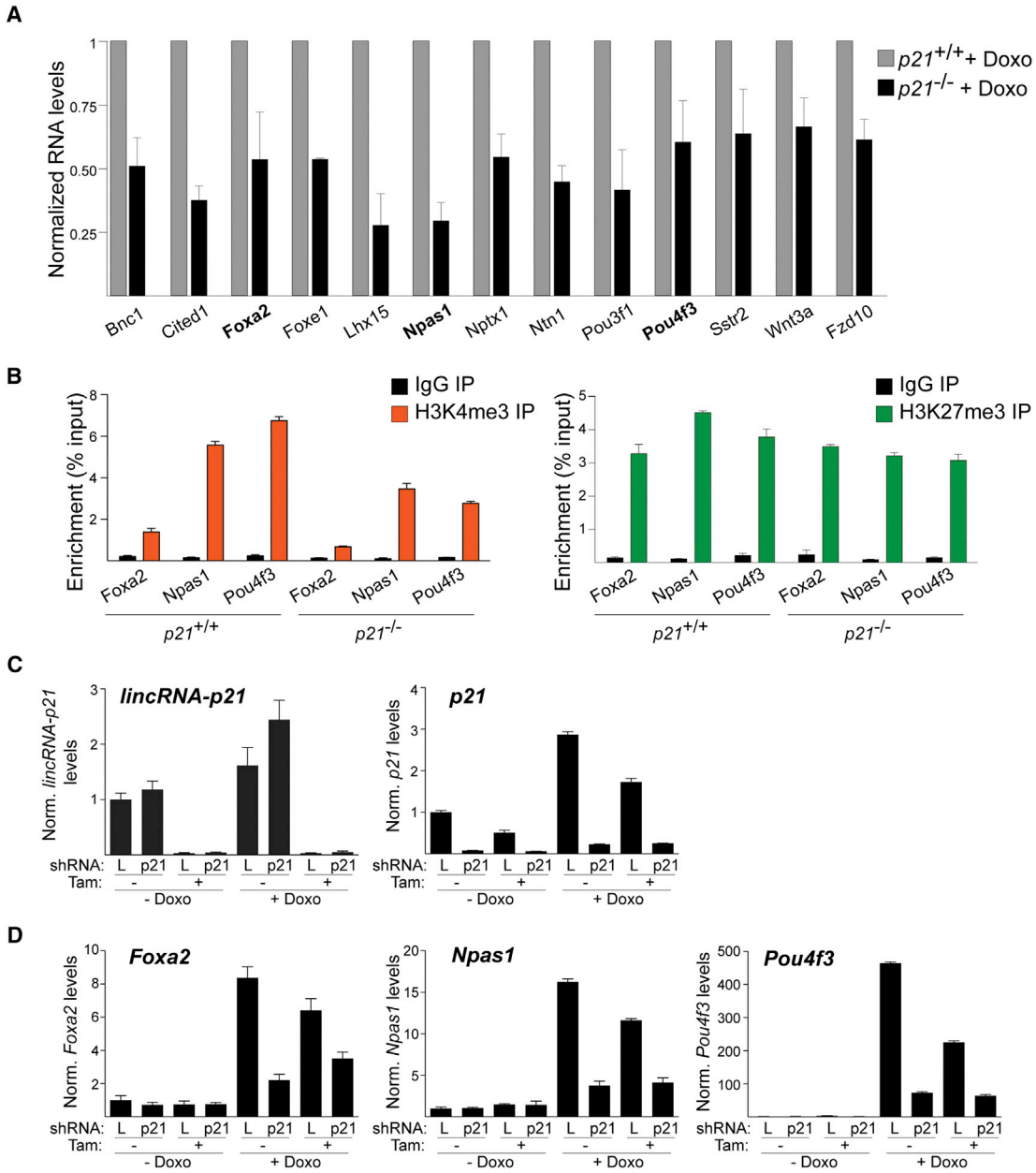

Figure 3. *LincRNA-p21* Regulates PRC2 Target Genes through *p21*

(A) Bar plot of normalized RNA levels of selected *lincRNA-p21*-regulated, PRC2 target genes in indicated cells, analyzed by qRT-PCR. Data are represented as mean ± SEM, n = 3.

(B) ChIP-qPCR analysis of the enrichment of H3K4me3 (left) and H3K27me3 (right) at the promoters of the indicated genes in doxorubicin-treated MEFs. Data, replicated in two independent experiments, are represented as mean ± SEM of technical replicates.

(C) qRT-PCR analysis of *lincRNA-p21* (left) and *p21* (right) in a *lincRNA-p21*$^{f/f}$; CreER^{T2} MEF line, infected with *p21*- or control *luciferase* (*L*)-specific shRNAs, harvested at 96 hr following mock treatment or tamoxifen (Tam)-mediated deletion of *lincRNA-p21* and at 24 hr following mock treatment or doxorubicin (Doxo)-induced DNA damage. Data are represented as mean ± SEM of technical replicates.

(D) qRT-PCR analysis of the effects of the treatments described in (C) on the expression levels of indicated *lincRNA-p21*-regulated, PRC2 target genes. Data were confirmed with an independent *p21*-targeting shRNA (data not shown).

See also Figure S5 and Table S4.

was formally possible that the observed defect in *p21* expression could be due to deletion of a previously unidentified enhancer element located within the targeted region or due to loss of other noncoding transcripts expressed from the *lincRNA-p21* locus. To address concerns with the specificity of the genetic model, we developed an independent approach to decrease

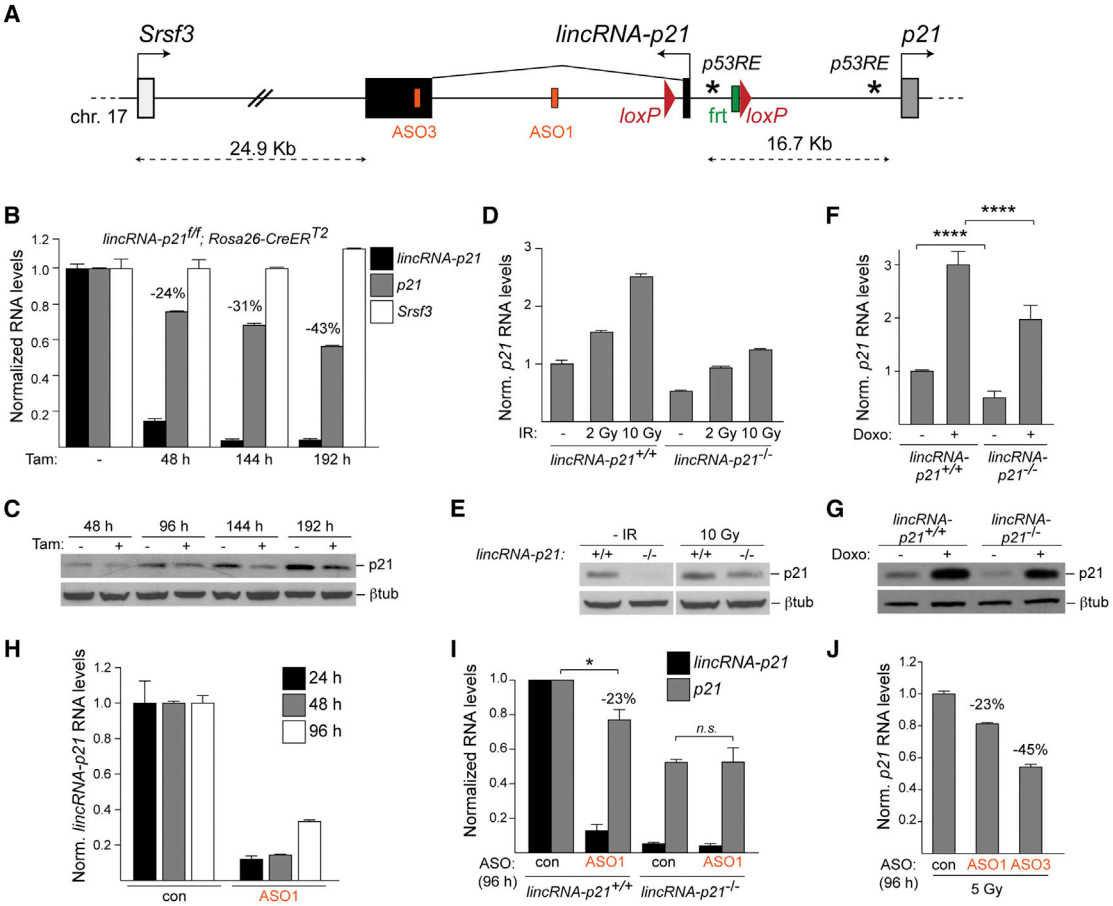

Figure 4. *LincRNA-p21* RNA Activates *p21*

(A) Schematic of the *lincRNA-p21*/*p21* locus, the targeting strategy, the positions of p53REs (*) in the promoters of *lincRNA-p21* and *p21*, and the target sequences of *lincRNA-p21*-specific ASO1 and ASO3.

(B) qRT-PCR analysis of *lincRNA-p21*, *p21*, and *Srsf3* RNA levels in indicated MEFs at indicated time-points after tamoxifen (Tam) treatment. Data, replicated in two independent experiments, are represented as mean ± SEM of technical replicates.

(C) Immunoblot analysis of *p21* protein levels in MEFs described in (B). β-tubulin was used as a loading control.

(D and E) qRT-PCR and immunoblot analysis of *p21* in MEFs of indicated genotypes, harvested 8 hr following treatment with the indicated doses of γ-irradiation (IR). Data, replicated in two independent experiments, are represented as mean ± SEM of technical replicates.

(F and G) qRT-PCR and immunoblot analysis of *p21* in MEFs of indicated genotypes, harvested untreated or 8 hr following doxorubicin (Doxo) treatment. Data are represented as mean ± SEM, n = 8, $p < 0.0001$, paired t test.

(H) qRT-PCR analysis of *lincRNA-p21* RNA levels at indicated time points following transfection with the indicated control nontargeting or *lincRNA-p21*-specific ASOs.

(I) qRT-PCR analysis of *p21* RNA levels at 96 hr following two consecutive ASO transfections, performed at a 48 hr interval, in MEFs of indicated genotypes. Data are represented as mean ± SEM, n = 4, $p = 0.0318$, paired t test.

(J) qRT-PCR analysis of *p21* RNA levels in ASO-treated wild-type MEFs, harvested 20 hr after 5 Gy irradiation. Data are represented as mean ± SEM of technical replicates.

See also Figure S6 and Table S4.

lincRNA-p21 levels using antisense oligonucleotides (ASOs), which can mediate efficient cotranscriptional knockdown of nuclear RNAs in an RNase H-dependent manner (Vickers et al., 2003). Transfection with two independent *lincRNA-p21*-specific ASOs, ASO1 and ASO3, led to greater than 90% loss of *lincRNA-p21* RNA levels at 24 hr following transfection, whereas ASO2 failed produce an efficient knockdown (Figures 4A, 4H, and S6B). The levels of inhibition diminished over time as MEFs underwent cell division and diluted the ASOs (Figure 4H). Using this approach, we found that at 96 hr following transfection with ASO1 and ASO3, the levels of *p21* were reproducibly reduced by 23% ± 9% compared to cells treated with a control, nontargeting ASO (Figures 4I and S6B). As a control for off-target effects, transfection of *lincRNA-p21*$^{-/-}$ MEFs with *lincRNA-p21*-specific ASOs did not further decrease *p21* levels (Figure 4I). We also observed that in the context of irradiation-induced DNA damage, transfection of wild-type MEFs with the two independent *lincRNA-p21*-specific ASOs led to a decrease in *p21* levels (23% and 45% with ASO1 and ASO3, respectively) (Figure 4J). Moreover, ASO-mediated *lincRNA-p21* depletion in the context

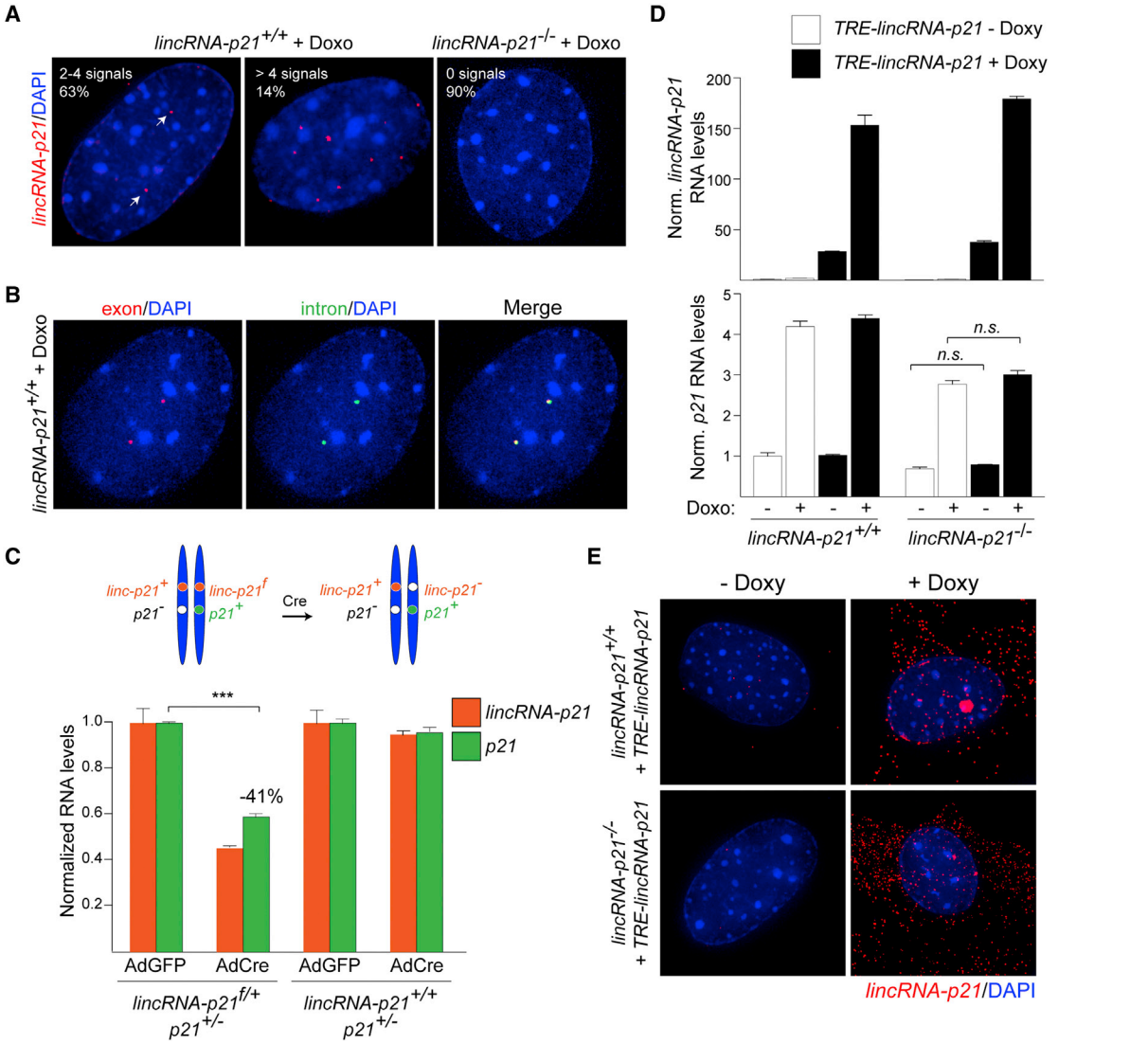

Figure 5. *LincRNA-p21* Regulates *p21* In *cis*

(A) Single-molecule RNA FISH detection of *lincRNA-p21* with exon-specific probes in indicated MEFs (white arrows). DNA was counterstained with DAPI. % represents the fraction of cells with indicated number of signals per cell (n = 150).

(B) Colocalization of exon- and intron-specific *lincRNA-p21* signals using single-molecule RNA FISH.

(C) (Top) Schematic. (Bottom) qRT-PCR analysis of *lincRNA-p21* and *p21* RNA levels in MEFs of indicated genotypes and treatments. Data are represented as mean ± SEM, n = 3, $p < 0.0001$, paired t test.

(D) qRT-PCR analysis of *lincRNA-p21* (top) and *p21* (bottom) RNA levels in MEFs of indicated genotypes, expressing TRE-*lincRNA-p21*, in the presence or absence of doxorubicin (Doxo) and doxycycline (Doxy). Data, replicated in two independent experiments, are represented as mean ± SEM of technical replicates.

(E) Single molecule RNA-FISH detection of exogenously expressed *lincRNA-p21* in (D).

See also Table S4.

of oncogenic stress (Feldser et al., 2010) similarly affected the expression of *p21* by 50% (Figure S6C). Collectively, these experiments point to a specific role for the *lincRNA-p21* transcript in the positive regulation of *p21* expression.

LincRNA-p21 Regulates *p21* In *cis*

Recent data suggest that lncRNAs can regulate nearby genes via either *cis*- or *trans*-acting mechanisms (Fatica and Bozzoni, 2014). To visualize *lincRNA-p21*, we performed single-molecule RNA FISH and observed that in wild-type MEFs treated with doxorubicin, *lincRNA-p21* localized exclusively to the nucleus, with 63% of the cells containing two or four prominent *lincRNA-p21* signals (Figure 5A). As a negative control, over 90% of *lincRNA-p21*$^{-/-}$ cells contained no detectable signals (Figure 5A). To test whether *lincRNA-p21* was localized at or near its site of transcription, we designed RNA FISH probes complementary to the intron of *lincRNA-p21*. Since introns are removed cotranscriptionally and quickly degraded, we reasoned

that the intron-specific RNA FISH signal should mark the genomic locus from which *lincRNA-p21* is expressed. In accordance with a *cis* model, we observed perfect colocalization between *lincRNA-p21* exonic and intronic signals in all wild-type cells, in which we could detect the short-lived intronic signal (Figure 5B).

To further distinguish between *cis* and *trans* mechanisms of action, we crossed *lincRNA-p21*$^{f/+}$ and *p21*$^{-/-}$ mice and isolated *lincRNA-p21*$^{f/+}$; *p21*$^{+/-}$ MEFs, in which *lincRNA-p21* and *p21* mutations were in *trans* (Figure 5C, top). In these cells, there was only one functional allele of *p21*, which was physically linked to a floxed allele of *lincRNA-p21*. We observed that upon adenoviral Cre-mediated deletion of the floxed allele of *lincRNA-p21*, the expression of *p21* from the same chromosome diminished by 41% ± 2% (Figure 5C, bottom), which is comparable to the decrease of *p21* levels in *lincRNA-p21*-deficient cells (Figure 4B). Thus, the wild-type allele of *lincRNA-p21* located in *trans* could not rescue *p21* levels. In control experiments, we confirmed that the altered *p21* expression required loss of *lincRNA-p21* (Figure 5C).

Consistent with a model in which *lincRNA-p21* acts on *p21* exclusively in *cis*, exogenous overexpression of *lincRNA-p21* failed to rescue *p21* levels in *lincRNA-p21*-deficient MEFs (Figure 5D). This is likely because the majority of the overexpressed RNA did not properly localize to the endogenous locus and was exported to the cytoplasm (Figure 5E).

LincRNA-p21 Recruits hnRNP-K to Promote p53-Dependent Transcription of *p21*

We next addressed the mechanism by which *lincRNA-p21* promoted *p21* expression. It has been established that *p21* is a direct target of p53, but several transcriptional coactivators have been implicated in the regulation of *p21* expression (Jung et al., 2010). In particular, studies in human cells have shown that one of these factors, hnRNP-K, binds to the *p21* promoter in response to DNA damage and promotes *p21* expression by recruiting p53 and/or by stabilizing p53 binding (Moumen et al., 2005). Since previous work had uncovered a direct interaction between *lincRNA-p21* and hnRNP-K (Huarte et al., 2010), we speculated that *lincRNA-p21* may be involved in mediating the coactivator function of hnRNP-K at the promoter of *p21*.

Consistent with previous data, we detected hnRNP-K and p53 at the p53RE in the *p21* promoter by ChIP-qPCR in doxorubicin-treated, wild-type cells, despite the low efficiency of hnRNP-K immunoprecipitation (less than 1%) (Figures 6A–6C and S7A). We next asked whether *lincRNA-p21* was required for the recruitment of hnRNP-K and p53 to the *p21* promoter. ChIP-qPCR of hnRNP-K revealed that the binding of hnRNP-K at the *p21* p53RE was reduced to background levels in *lincRNA-p21*-deficient MEFs (Figure 6B). Moreover, as expected in the absence of proper localization of hnRNP-K at this site, we observed by ChIP-qPCR that the strength of p53 binding at the *p21* promoter was diminished by 43% ± 12% in *lincRNA-p21*-deficient cells compared to wild-type controls (Figure 6C). Reduced binding of p53 at the *p21* promoter was also observed in MEFs in which *lincRNA-p21* RNA levels were downregulated by two independent *lincRNA-p21*-specific ASOs (ASO1 and ASO3) compared to a control, nontargeting ASO, whereas ASO2, which does not lead to efficient *lincRNA-p21* downregulation (Figure S6B), did not alter p53 binding (Figure 6D). These data suggested that *lincRNA-p21* RNA is required for the recruitment of hnRNP-K to the p53RE in the promoter of *p21* and for the efficient binding of p53 at this site.

In line with a model whereby *lincRNA-p21* and hnRNP-K cooperate to promote *p21* transcription, knockdown of hnRNP-K led to diminished *p21* levels in doxorubicin-treated *lincRNA-p21*$^{+/+}$ MEFs but not in *lincRNA-p21*$^{-/-}$ MEFs (Figures 6E and 6F). Of note, hnRNP-K downregulation also resulted in reduced *lincRNA-p21* levels, suggesting that hnRNP-K is required for the induction and/or stability of *lincRNA-p21* (Figure 6G).

LincRNA-p21 Regulates the G1/S Checkpoint, Proliferation Rates, and Reprogramming Efficiency

Finally, we investigated the physiological consequences of *lincRNA-p21* deficiency in MEFs. Based on its role in regulating *p21*, which is a major mediator of checkpoint function in the p53 pathway, we anticipated that *lincRNA-p21* deletion might affect the G1/S checkpoint. To test for this, we assayed the proportion of cells that entered S phase following γ-irradiation in *lincRNA-p21*-proficient and -deficient cells. Compared to control cells, a significantly elevated fraction of *lincRNA-p21*$^{-/-}$ MEFs as well as MEFs transfected with *lincRNA-p21*-specific ASOs, continued to incorporate BrdU in the presence of DNA damage (Figure 7A). This phenotype was comparable to the G1/S checkpoint defect observed in p21-deficient MEFs (Figure S7B). We concluded that the G1/S checkpoint was indeed compromised in the absence of *lincRNA-p21*.

Consistent with a defective checkpoint function, we reproducibly observed that *lincRNA-p21*-deficient MEFs proliferated faster compared to wild-type controls, which is similar to *p21*$^{-/-}$ cells (Figures 7B and S7C). Moreover, we observed that *lincRNA-p21* deficiency significantly increased the reprogramming efficiency of primary MEFs, as indicated by enhanced levels of the pluripotency marker Nanog and an increased number of alkaline phosphatase-positive colonies in *lincRNA-p21*$^{-/-}$ compared to littermate, wild-type MEFs (Figures 7C and 7D).

In contrast, we did not find a role for *lincRNA-p21* in other well-characterized functions of the p53 pathway in MEFs, including apoptosis, the ability to promote senescence following prolonged exposure to doxorubicin-induced DNA damage, and the capacity to inhibit cellular transformation (Figures S7D–S7F). These data are consistent with p21 not playing a role in these processes (Pantoja and Serrano, 1999). In sum, these data indicate that loss of *lincRNA-p21* leads to cellular phenotypes similar to the consequences of *p21* deletion in MEFs.

DISCUSSION

An emerging class of lncRNAs, including *lincRNA-p21*, has been proposed to regulate the expression of multiple genes in *trans* (Fatica and Bozzoni, 2014). For the most part, these studies rely on global gene expression profiling, which identifies hundreds, sometimes thousands, of differentially expressed genes in cells with RNAi-mediated knockdown or genetic depletion of lncRNAs. From a mechanistic perspective, however, it is

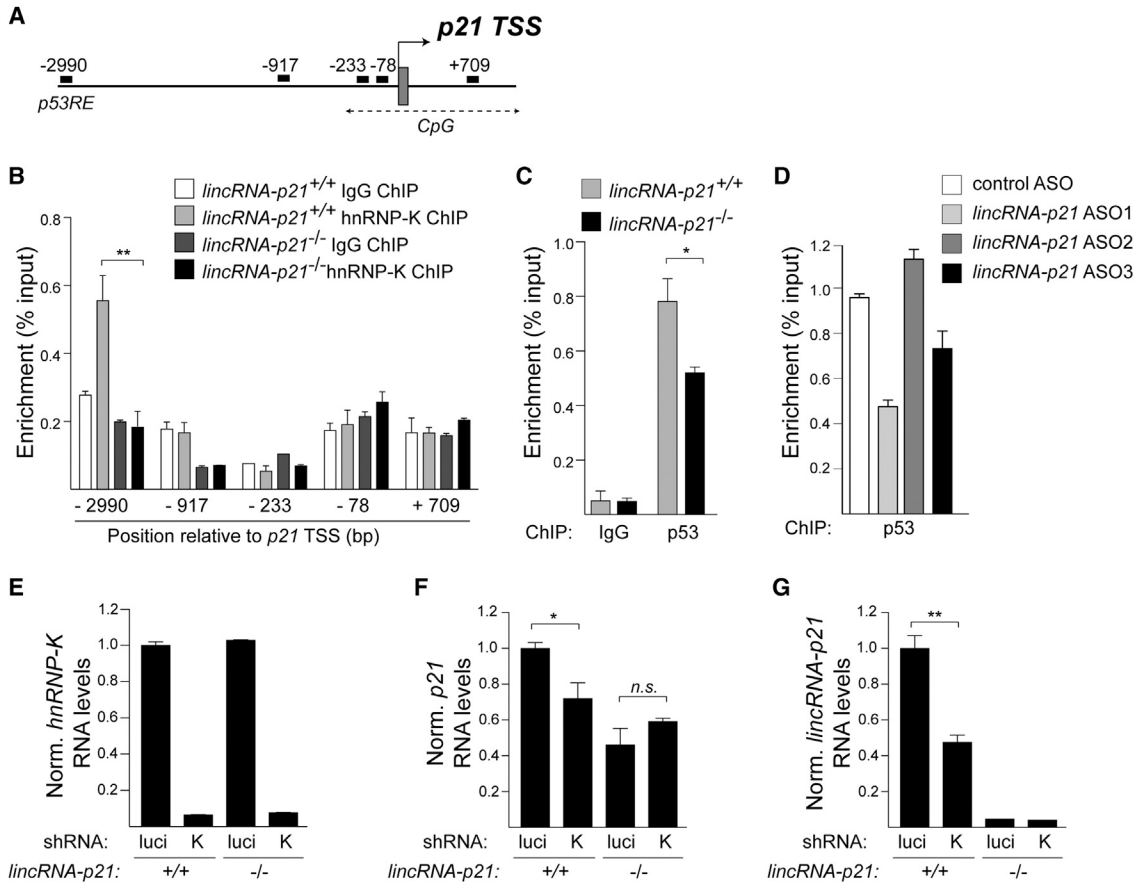

Figure 6. *LincRNA-p21* Acts with hnRNP-K as a Transcriptional Coactivator of p53-Mediated Expression of *p21*

(A) Schematic of the positions of qPCR primers used for ChIP analysis, indicating the distance (base pairs) relative to the *p21* transcription start site (TSS).

(B) A representative hnRNP-K ChIP-qPCR analysis in indicated MEF lines, harvested 8 hr following doxorubicin treatment. Data, replicated in four independent experiments, are represented as mean ± SEM of technical replicates (n = 4, p = 0.0020, paired t test).

(C) A representative p53 ChIP-qPCR analysis using the −2,990 (p53RE) primer set in indicated MEF lines, harvested 8 hr following doxorubicin treatment. Data, replicated in three independent experiments, are represented as mean ± SEM of technical replicates (n = 3, p = 0.043, paired t test).

(D) ChIP-qPCR analysis of the relative p53 binding at the −2,990 (p53RE) site of the *p21* promoter in ASO-treated wild-type MEFs. Data are represented as mean ± SEM of technical replicates.

(E–G) qRT-PCR analysis of (E) hnRNP-K, (F) *p21* (mean ± SEM, n = 4, p = 0.0326, paired t test), and (G) *lincRNA-p21* (mean ± SEM, n = 3, p = 0.0030, paired t test) levels in indicated MEFs, expressing luciferase (luci) or hnRNP-K (K)-specific shRNAs, harvested at 8 hr following doxorubicin treatment.

See also Figure S7A and Table S4.

important to differentiate direct targets of lncRNA regulation from genes that are indirectly affected by lncRNA loss. For instance, we found by global expression analysis that genetic deletion of *lincRNA-p21* in primary MEFs led to the deregulation of close to 1,000 genes. However, we present several lines of evidence that do not support widespread *trans*-regulatory activity of this lincRNA. First, single-molecule RNA FISH revealed that *lincRNA-p21* did not interact with multiple distinct loci but was localized primarily at or near its transcription site. Next, we did not find evidence of nuclear domains near the *lincRNA-p21* locus that cluster *lincRNA-p21*-regulated genes (Engreitz et al., 2013). Finally, the low copy number (~8 *lincRNA-p21* molecules/cell) does not support a global function for *lincRNA-p21* as a protein-binding partner. For these reasons, we believe it unlikely that *lincRNA-p21* has genome-wide regulatory functions.

The discrepancy with previous functional studies, which have proposed global nuclear and cytosolic *trans* functions for *lincRNA-p21* (Huarte et al., 2010; Yang et al., 2014; Yoon et al., 2012), can likely be attributed to the different methods used to perform loss-of-function analyses (genetic deletion versus RNAi) and to the different cell types (MEFs versus human cancer cell lines). Importantly, a genetic deletion, rather than an RNAi approach, was required to unveil the *cis* function of *lincRNA-p21* in the regulation of *p21*. Additional advantages of using a conditional knockout mouse model include specificity, efficiency, and opportunity to study the long-term consequences of *lincRNA-p21* depletion in vitro and in vivo.

Using our genetic approach, we present compelling evidence that *lincRNA-p21* activates the expression of its neighboring gene *p21* by 30%–50%. As several of the major phenotypes of

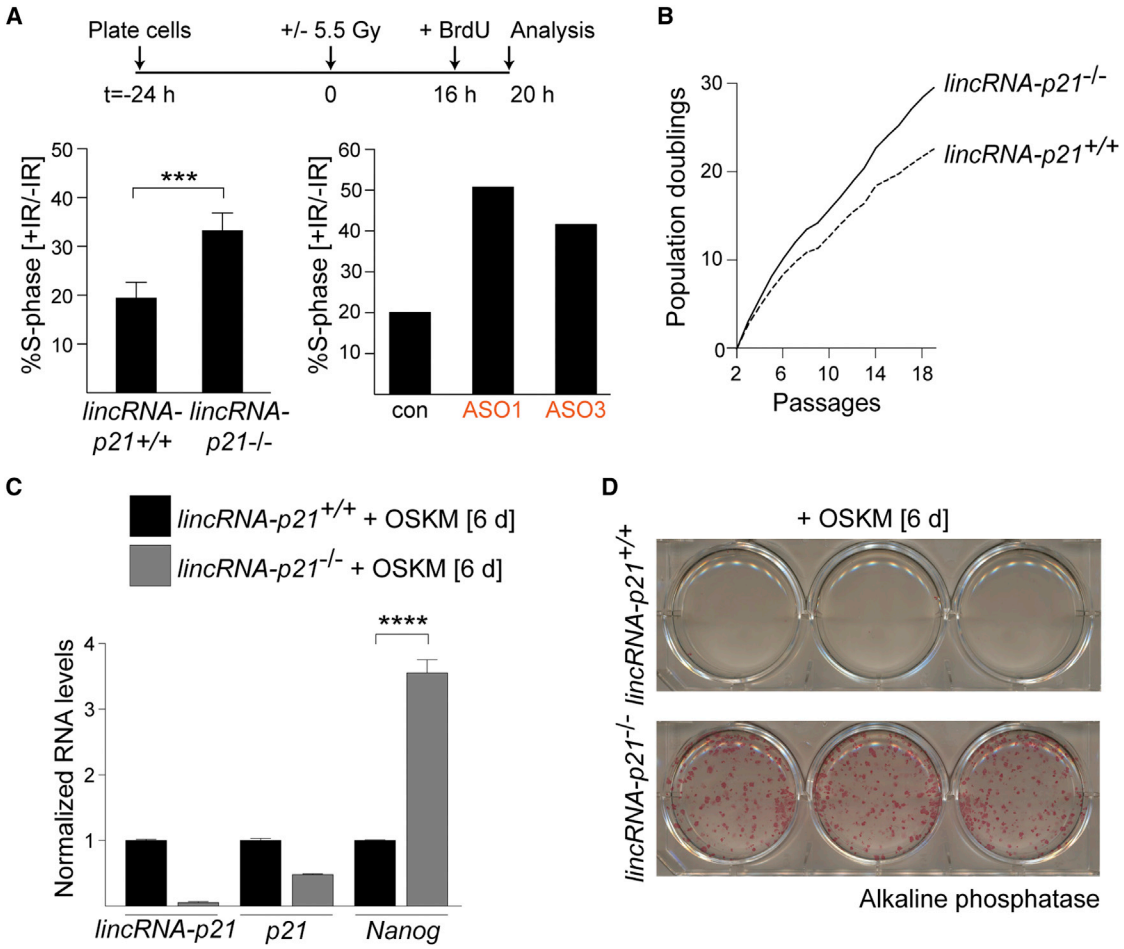

Figure 7. *LincRNA-p21* Controls the G1/S Checkpoint, Proliferation, and the Induction of Pluripotency

(A) (Top) Schematic of the G1/S checkpoint assay. (Bottom, left) FACS analysis of the fraction of BrdU-positive cells in irradiated samples relative to untreated cells. Data are represented as mean ± SEM, n = 4, p = 0.0060, paired t test. (Bottom, right) FACS analysis of the fraction of BrdU-positive cells in wild-type samples, transfected with the indicated ASOs.

(B) Proliferation of *lincRNA-p21*$^{+/+}$ and *lincRNA-p21*$^{-/-}$ MEFs isolated from littermates. Data are representative of three independent growth curve analyses.

(C) qRT-PCR analysis of *lincRNA-p21*, *p21*, and *Nanog* levels in RNA harvested from *lincRNA-p21*-proficient and -deficient cells at 6 days following infection with the reprogramming factors Oct4, Sox2, Klf4, and Myc (OSKM). Data are represented as mean ± SEM, n = 3, p = 0.0004, paired t test.

(D) Images of alkaline phosphatase-positive colonies stained 6 days following infection of MEFs with indicated genotypes with OSKM.

See also Figures S7B–S7F and Table S4.

lincRNA-p21 deficiency could be replicated by two independent *lincRNA-p21*-targeting ASOs, we conclude that this enhancer-like phenotype is mediated by the *lincRNA-p21* transcript and not through a genetic element located in the region of deletion. These data also argue against a role for another RNA species expressed from the *lincRNA-p21* locus in these phenotypes and overcome concerns about nonspecific consequences of altered chromatin architecture in mutant cells. Of note, the *lincRNA-p21* locus does not bear the high H3K4me1/H3K4me3 ratio indicative of enhancer elements, and *lincRNA-p21* RNA has a half-life in the range of hours, rather than minutes, both of which suggest that *lincRNA-p21* likely does not belong to the recently described class of eRNAs (Ørom and Shiekhattar, 2011). However, we cannot exclude the possibility that *lincRNA-p21* may arise from an enhancer region (Melo et al., 2013b).

Importantly, we formally show that *lincRNA-p21* regulates *p21* in *cis*. This conclusion is substantiated by a genetic experiment in which we place *lincRNA-p21* and *p21* mutations in *trans* as well as by the predominant two-dot nuclear pattern of *lincRNA-p21* by RNA FISH and by the inability to rescue phenotypes of *lincRNA-p21* deficiency by exogenous expression of *lincRNA-p21*. Consistent with our finding of *cis* regulation, the majority of the cellular phenotypes and expression changes observed in *lincRNA-p21*-deficient cells could be attributed to the role of *lincRNA-p21* in activating *p21*, including defects in the G1/S cell-cycle checkpoint and in proliferation control. Conversely, *p21*-independent functions of the p53 pathway in MEFs, including the abilities to promote apoptosis and senescence and the capacity to inhibit oncogene-mediated cellular transformation, were not affected by loss of *lincRNA-p21*. The

lack of an overt organismal phenotype in *lincRNA-p21*-deficient mice is also in agreement with a *cis* regulatory model, given that p21-deficient animals develop normally and exhibit only mild susceptibility to tumor development with a long average latency (Martín-Caballero et al., 2001).

In further support of a *cis* regulatory model, we provide direct evidence that the regulation of a subset of PRC2 target genes by *lincRNA-p21* is mediated through *p21*. This observation reveals a function of the p53 pathway. It remains to be determined what the physiological purpose of derepression of PRC2 targets in response to prolonged genotoxic stress may be. One potential function could be the elimination of damaged cells by promoting terminal differentiation through the expression of multiple lineage-specific factors. This model is consistent with a growing body of literature that has linked *p21* function in growth arrest with cellular differentiation and organism development (Muñoz-Espín et al., 2013). Moreover, this phenomenon might be related to the increased reprogramming rates observed in p53-, p21-, *and lincRNA-p21*-deficient primary MEFs (Hanna et al., 2009; Kawamura et al., 2009). Whereas this phenotype was originally attributed to increased cellular proliferation rates, cell-intrinsic factors were also acknowledged as potential modulators of the transition to a pluripotency state (Hanna et al., 2009).

The data presented here indicate that *lincRNA-p21* acts in concert with hnRNP-K to promote p53-mediated expression of *p21*. Our findings support a model in which *lincRNA-p21* and hnRNP-K act as transcriptional coactivators for local p53-mediated transcription. We propose that hnRNP-K binds directly to *lincRNA-p21*, which serves to promote the stability of *lincRNA-p21* as well as to target hnRNP-K to the *p21* locus. In the presence of *lincRNA-p21* and hnRNP-K, p53 can carry out efficient induction of *p21*. These findings are consistent with previous studies in human cells that have implicated hnRNP-K as a transcriptional coactivator for p53-mediated expression of *p21* (Moumen et al., 2005). An intriguing question is how *lincRNA-p21* deficiency, which affects *p21* expression levels by only 30%–50%, leads to the range and extent of phenotypes that are comparable to complete loss of *p21*. We propose that *lincRNA-p21*-mediated reinforcement of activation may push *p21* past a threshold for response and thus facilitate finer regulation of cellular responses.

It is important to understand the role of reinforcing *p21* expression in *cis*. We speculate that this may be key in the context of the p53 tumor suppressor pathway, which is complex and whose outcome can be specific to cell type and context (Vousden and Prives, 2009). *p21* and hundreds of other genes are activated by p53 in response to stress, and different targets have been shown to dictate different cellular outcomes (Levine and Oren, 2009). Thus, a function of *lincRNA-p21* and hnRNP-K may be to locally amplify the execution of a specific p53-dependent transcription output, reliant on sustained *p21* activation. The contribution of *lincRNA-p21* is to recruit hnRNP-K in a locus-restricted manner and to maintain *p21* activation.

In summary, these data point to *lincRNA-p21* as a key modulator of gene expression in the p53 pathway, influencing the activation and the chromatin state of hundreds of genes through its *cis* control of *p21* expression. This work highlights the power of using defined genetic systems to dissect the contribution of lncRNAs to complex biological pathways. The model presented here has general implications for how low copy number, *cis*-acting lncRNAs may locally reinforce the specificity of broad transcriptional programs.

EXPERIMENTAL PROCEDURES

Mouse Strains, Cell Culture, and Treatments

LincRNA-p21 floxed and null mice and E13.5 MEFs were generated as described in Supplemental Experimental Procedures. Rosa26-CreER^{T2} (Ventura et al., 2007) and *p21* mice (Jackson Laboratory, stock number 003263) have previously been described (Brugarolas et al., 1995). The Massachusetts Institute of Technology (MIT) Institutional Animal Care and Use Committee approved all animal studies and procedures.

To delete *lincRNA-p21* in *lincRNA-p21*$^{f/f}$; Rosa26-CreER^{T2} MEFs, cells were treated with 0.5 μM 4-OHT. To delete *lincRNA-p21* in *lincRNA-p21*$^{f/+}$; *p21*$^{+/-}$ MEFs, cells were infected two times at a 24 hr interval with Cre recombinase or control GFP adenovirus. To induce DNA damage, cells were treated with 0.5 μM doxorubicin or irradiated with 2 or 10 Gy of γ-irradiation and harvested at indicated time points following treatment.

5-10-5 MOE gapmer oligonucleotides were designed and generously provided by Isis Pharmaceuticals (Table S4). A total of 1 μM *lincRNA-p21*-specific or nontargeting control ASOs were transfected twice at a 48 hr interval into 1 × 10^6 *lincRNA-p21*$^{+/+}$ and *lincRNA-p21*$^{-/-}$ MEFs using the Amaxa Mouse/Rat Hepatocyte Nucleofector Kit (Lonza) and the Nucleofector 2b Device (Lonza).

Constructs

Full-length mouse *lincRNA-p21* cDNA (a gift from John Rinn) was expressed from the pSLIK lentiviral expression system (Shin et al., 2006). pLKO p21 and hnRNP-K hairpins were purchased from The RNA Consortium (TRC) collection (Thermo Scientific) (p21, clone IDs TRCN0000042583 [sh#1] and TRCN0000042584 [sh#2, used to replicate data]; hnRNP-K: TRCN0000096825 [sh#4]). Lentivirus was produced as described in Supplemental Experimental Procedures.

RNA Isolation and RT-qPCR

RNA was isolated with RNeasy Mini Kit (QIAGEN) and reverse transcribed using High Capacity cDNA Reverse Transcription Kit (Applied Biosystems). SYBR Green PCR master mix (Applied Biosystems) was used for qPCR with primers listed in Table S4. Expression levels were calculated relative to GAPDH and normalized to control samples.

Western Blotting

Western blotting was performed with whole-cell lysates, using the following antibodies: p21 (clone F-5, sc-6246, Santa Cruz Biotechnology), hnRNP-K (ab70492, Abcam), H3K4me3 (ab8580, Abcam), H3K27me3 (ab6002, Abcam), and loading control β-tubulin (ab6046, Abcam).

Chromatin Immunoprecipitation

Chromatin immunoprecipitation (ChIP) was performed as described in Supplemental Experimental Procedures with the following antibodies: H3K4me3 (ab8580, Abcam), H3K27me3 (ab6002, Abcam), p53 (clone CM5, VP-P956, Vector Laboratories), hnRNP-K (ab70492, Abcam), and control IgG (ChIP grade, ab46540, Abcam). DNA was submitted for high-throughput sequencing (ChIP-seq) or used for qPCR analysis (ChIP-qPCR) using primers listed in Table S4. The data represent the percentage of input that was immunoprecipitated.

Single-Molecule RNA-Fluorescence In Situ Hybridization

Single-molecule RNA FISH was performed as previously described (Raj et al., 2008) with probes listed in Table S4.

G1/S Checkpoint Assay

The G1/S checkpoint assay was performed as previously described (Brugarolas et al., 1995) with modifications (see Supplemental Experimental Procedures). The data represent the fraction of BrdU-positive cells in irradiated samples relative to nonirradiated samples for each cell line.

ACCESSION NUMBERS

All primary RNA-seq and ChIP-seq data are available at Gene Expression Omnibus under accession number GSE52958.

SUPPLEMENTAL INFORMATION

Supplemental Information includes seven figures, four tables, and Supplemental Experimental Procedures and can be found with this article at http://dx.doi.org/10.1016/j.molcel.2014.04.025.

ACKNOWLEDGMENTS

We thank John Rinn, Vasilena Gocheva, and Thales Papagiannakopoulos for critical review of the manuscript. We are extremely grateful to Dirk Hockemeyer (UC Berkeley) for technical assistance and reagents related to the reprogramming experiment and to Jerry Ruth (Biosearch Technologies) for generously providing RNA FISH reagents. We are grateful to Aurora Burds O'Connor from the Rippel Mouse ES Cell and Transgenics Facility of the Swanson Biotechnology Center. This work was supported by NIH (T.J.), the Howard Hughes Medical Institute, and the Ludwig Center for Molecular Oncology at MIT. N.D. was supported by a Damon Runyon Fellowship Award. T.J. is the David H. Koch Professor of Biology and a Daniel K. Ludwig Scholar at MIT. The authors wish to dedicate this paper to the memory of Officer Sean Collier, for his caring service to the MIT community and for his sacrifice.

Received: December 11, 2013
Revised: March 4, 2014
Accepted: April 15, 2014
Published: May 22, 2014

REFERENCES

Aldiri, I., and Vetter, M.L. (2012). PRC2 during vertebrate organogenesis: a complex in transition. Dev. Biol. *367*, 91–99.

Brugarolas, J., Chandrasekaran, C., Gordon, J.I., Beach, D., Jacks, T., and Hannon, G.J. (1995). Radiation-induced cell cycle arrest compromised by p21 deficiency. Nature *377*, 552–557.

Davidovich, C., Zheng, L., Goodrich, K.J., and Cech, T.R. (2013). Promiscuous RNA binding by Polycomb repressive complex 2. Nat. Struct. Mol. Biol. *20*, 1250–1257.

Deng, C., Zhang, P., Harper, J.W., Elledge, S.J., and Leder, P. (1995). Mice lacking p21 CIP1/WAF1 undergo normal development, but are defective in G1 checkpoint control. Cell *82*, 675–684.

Engreitz, J.M., Pandya-Jones, A., McDonel, P., Shishkin, A., Sirokman, K., Surka, C., Kadri, S., Xing, J., Goren, A., Lander, E.S., et al. (2013). The Xist lncRNA exploits three-dimensional genome architecture to spread across the X chromosome. Science *341*, 1237973.

Fatica, A., and Bozzoni, I. (2014). Long non-coding RNAs: new players in cell differentiation and development. Nat. Rev. Genet. *15*, 7–21.

Feldser, D.M., Kostova, K.K., Winslow, M.M., Taylor, S.E., Cashman, C., Whittaker, C.A., Sanchez-Rivera, F.J., Resnick, R., Bronson, R., Hemann, M.T., and Jacks, T. (2010). Stage-specific sensitivity to p53 restoration during lung cancer progression. Nature *468*, 572–575.

Guttman, M., Amit, I., Garber, M., French, C., Lin, M.F., Feldser, D., Huarte, M., Zuk, O., Carey, B.W., Cassady, J.P., et al. (2009). Chromatin signature reveals over a thousand highly conserved large non-coding RNAs in mammals. Nature *458*, 223–227.

Hanna, J., Saha, K., Pando, B., van Zon, J., Lengner, C.J., Creyghton, M.P., van Oudenaarden, A., and Jaenisch, R. (2009). Direct cell reprogramming is a stochastic process amenable to acceleration. Nature *462*, 595–601.

Huarte, M., Guttman, M., Feldser, D., Garber, M., Koziol, M.J., Kenzelmann-Broz, D., Khalil, A.M., Zuk, O., Amit, I., Rabani, M., et al. (2010). A large intergenic noncoding RNA induced by p53 mediates global gene repression in the p53 response. Cell *142*, 409–419.

Hung, T., Wang, Y., Lin, M.F., Koegel, A.K., Kotake, Y., Grant, G.D., Horlings, H.M., Shah, N., Umbricht, C., Wang, P., et al. (2011). Extensive and coordinated transcription of noncoding RNAs within cell-cycle promoters. Nat. Genet. *43*, 621–629.

Jung, Y.S., Qian, Y., and Chen, X. (2010). Examination of the expanding pathways for the regulation of p21 expression and activity. Cell. Signal. *22*, 1003–1012.

Kaneko, S., Son, J., Shen, S.S., Reinberg, D., and Bonasio, R. (2013). PRC2 binds active promoters and contacts nascent RNAs in embryonic stem cells. Nat. Struct. Mol. Biol. *20*, 1258–1264.

Kawamura, T., Suzuki, J., Wang, Y.V., Menendez, S., Morera, L.B., Raya, A., Wahl, G.M., and Izpisúa Belmonte, J.C. (2009). Linking the p53 tumour suppressor pathway to somatic cell reprogramming. Nature *460*, 1140–1144.

Khalil, A.M., Guttman, M., Huarte, M., Garber, M., Raj, A., Rivea Morales, D., Thomas, K., Presser, A., Bernstein, B.E., van Oudenaarden, A., et al. (2009). Many human large intergenic noncoding RNAs associate with chromatin-modifying complexes and affect gene expression. Proc. Natl. Acad. Sci. USA *106*, 11667–11672.

Lee, J.T., and Bartolomei, M.S. (2013). X-inactivation, imprinting, and long noncoding RNAs in health and disease. Cell *152*, 1308–1323.

Levine, A.J., and Oren, M. (2009). The first 30 years of p53: growing ever more complex. Nat. Rev. Cancer *9*, 749–758.

Marín-Béjar, O., Marchese, F.P., Athie, A., Sánchez, Y., González, J., Segura, V., Huang, L., Moreno, I., Navarro, A., Monzó, M., et al. (2013). Pint lincRNA connects the p53 pathway with epigenetic silencing by the Polycomb repressive complex 2. Genome Biol. *14*, R104.

Martín-Caballero, J., Flores, J.M., García-Palencia, P., and Serrano, M. (2001). Tumor susceptibility of p21(Waf1/Cip1)-deficient mice. Cancer Res. *61*, 6234–6238.

Melo, C.A., Drost, J., Wijchers, P.J., van de Werken, H., de Wit, E., Oude Vrielink, J.A., Elkon, R., Melo, S.A., Léveillé, N., Kalluri, R., et al. (2013a). eRNAs are required for p53-dependent enhancer activity and gene transcription. Mol. Cell *49*, 524–535.

Melo, C.A., Léveillé, N., and Agami, R. (2013b). eRNAs reach the heart of transcription. Cell Res. *23*, 1151–1152.

Missero, C., Di Cunto, F., Kiyokawa, H., Koff, A., and Dotto, G.P. (1996). The absence of p21 Cip1/WAF1 alters keratinocyte growth and differentiation and promotes ras-tumor progression. Genes Dev. *10*, 3065–3075.

Moumen, A., Masterson, P., O'Connor, M.J., and Jackson, S.P. (2005). hnRNP K: an HDM2 target and transcriptional coactivator of p53 in response to DNA damage. Cell *123*, 1065–1078.

Muñoz-Espín, D., Cañamero, M., Maraver, A., Gómez-López, G., Contreras, J., Murillo-Cuesta, S., Rodríguez-Baeza, A., Varela-Nieto, I., Ruberte, J., Collado, M., and Serrano, M. (2013). Programmed cell senescence during mammalian embryonic development. Cell *155*, 1104–1118.

Ørom, U.A., and Shiekhattar, R. (2011). Long non-coding RNAs and enhancers. Curr. Opin. Genet. Dev. *21*, 194–198.

Pantoja, C., and Serrano, M. (1999). Murine fibroblasts lacking p21 undergo senescence and are resistant to transformation by oncogenic Ras. Oncogene *18*, 4974–4982.

Purvis, J.E., Karhohs, K.W., Mock, C., Batchelor, E., Loewer, A., and Lahav, G. (2012). p53 dynamics control cell fate. Science *336*, 1440–1444.

Raj, A., van den Bogaard, P., Rifkin, S.A., van Oudenaarden, A., and Tyagi, S. (2008). Imaging individual mRNA molecules using multiple singly labeled probes. Nat. Methods *5*, 877–879.

Rinn, J.L., and Chang, H.Y. (2012). Genome regulation by long noncoding RNAs. Annu. Rev. Biochem. *81*, 145–166.

Shin, K.J., Wall, E.A., Zavzavadjian, J.R., Santat, L.A., Liu, J., Hwang, J.I., Rebres, R., Roach, T., Seaman, W., Simon, M.I., and Fraser, I.D. (2006). A single lentiviral vector platform for microRNA-based conditional RNA interference and coordinated transgene expression. Proc. Natl. Acad. Sci. USA *103*, 13759–13764.

Steinman, R.A., Hoffman, B., Iro, A., Guillouf, C., Liebermann, D.A., and el-Houseini, M.E. (1994). Induction of p21 (WAF-1/CIP1) during differentiation. Oncogene *9*, 3389–3396.

Subramanian, A., Tamayo, P., Mootha, V.K., Mukherjee, S., Ebert, B.L., Gillette, M.A., Paulovich, A., Pomeroy, S.L., Golub, T.R., Lander, E.S., and Mesirov, J.P. (2005). Gene set enrichment analysis: a knowledge-based approach for interpreting genome-wide expression profiles. Proc. Natl. Acad. Sci. USA *102*, 15545–15550.

Ventura, A., Kirsch, D.G., McLaughlin, M.E., Tuveson, D.A., Grimm, J., Lintault, L., Newman, J., Reczek, E.E., Weissleder, R., and Jacks, T. (2007). Restoration of p53 function leads to tumour regression in vivo. Nature *445*, 661–665.

Vickers, T.A., Koo, S., Bennett, C.F., Crooke, S.T., Dean, N.M., and Baker, B.F. (2003). Efficient reduction of target RNAs by small interfering RNA and RNase H-dependent antisense agents. A comparative analysis. J. Biol. Chem. *278*, 7108–7118.

Vousden, K.H., and Prives, C. (2009). Blinded by the Light: The Growing Complexity of p53. Cell *137*, 413–431.

Yang, F., Zhang, H., Mei, Y., and Wu, M. (2014). Reciprocal regulation of HIF-1α and lincRNA-p21 modulates the Warburg effect. Mol. Cell *53*, 88–100.

Yoon, J.H., Abdelmohsen, K., Srikantan, S., Yang, X., Martindale, J.L., De, S., Huarte, M., Zhan, M., Becker, K.G., and Gorospe, M. (2012). LincRNA-p21 suppresses target mRNA translation. Mol. Cell *47*, 648–655.

Zhang, P., Wong, C., Liu, D., Finegold, M., Harper, J.W., and Elledge, S.J. (1999). p21 (CIP1) and p57(KIP2) control muscle differentiation at the myogenin step. Genes Dev. *13*, 213–224.

Zhao, J., Ohsumi, T.K., Kung, J.T., Ogawa, Y., Grau, D.J., Sarma, K., Song, J.J., Kingston, R.E., Borowsky, M., and Lee, J.T. (2010). Genome-wide identification of polycomb-associated RNAs by RIP-seq. Mol. Cell *40*, 939–953.